

# Plant Cuticular Lipid Export Requires an ABC Transporter

Jamie A. Pighin,<sup>1\*</sup> Huanquan Zheng,<sup>1\*</sup> Laura J. Balakshin,<sup>1</sup>  
Ian P. Goodman,<sup>1</sup> Tamara L. Western,<sup>1</sup> Reinhard Jetter,<sup>1,2</sup>  
Ljerka Kunst,<sup>1</sup> A. Lacey Samuels<sup>1†</sup>

A waxy protective cuticle coats all primary aerial plant tissues. Its synthesis requires extensive export of lipids from epidermal cells to the plant surface. *Arabidopsis cer5* mutants had reduced stem cuticular wax loads and accumulated sheetlike inclusions in the cytoplasm of wax-secreting cells. These inclusions represented abnormal deposits of cuticular wax and resembled inclusions found in a human disorder caused by a defective peroxisomal adenosine triphosphate binding cassette (ABC) transporter. We found that the *CER5* gene encodes an ABC transporter localized in the plasma membrane of epidermal cells and conclude that it is required for wax export to the cuticle.

All primary aerial organs of land plants are covered with a waxy cuticle that is essential for their protection and interaction with the environment. The cuticle is composed of very-long-chain fatty acids and their derivatives, collectively termed cuticular wax, embedded within and encasing the cutin matrix (1). Cuticle synthesis requires extensive transport of lipids out of the epidermal cells to the plant surface. The mechanism of export of the cuticular lipids is unknown.

To identify mutants defective in lipid transport to the cuticle, we examined a collection of *Arabidopsis thaliana eceriferum* (or *cer*) lines for changes in wax-secreting epidermal cells by transmission electron microscopy (TEM). *Cer* mutants have a glossy, bright green stem phenotype because of a reduction or altered composition of cuticular wax (2). TEM study (3) of the stem epidermis of the *cer5* mutant revealed an unusual cellular phenotype. Similar to the wild type, *cer5* cells were entirely filled with a central vacuole with the cytoplasm present in a thin rim around the edge of the cell (Fig. 1A), but they also contained large protrusions of cytoplasm into the vacuole (Fig. 1B). Within these protrusions, loose bundles of linear inclusions, distinct from the endoplasmic reticulum, Golgi, and cytoskeletal elements, were found (Fig. 1C). These inclusions were found only in the epidermis; they were never observed in other cell types. Morphologically similar trilamellar inclusions had been described in the cells of patients with X-linked adrenoleukodystrophy (ALD), a neurodegenerative disease caused by a defect in an ABC transporter involved in transport of saturated

very-long-chain fatty acids into the peroxisome for  $\beta$ -oxidation (4).

The *cer5* stem epidermis was further examined by cryo-scanning electron microscopy (SEM) (Fig. 1D) (3). The stem surface was sparsely covered with epicuticular wax crystals, consistent with reports that the wax load on *cer5* stems is merely reduced, not eliminated (5). The *cer5* epidermal cells contained large sheetlike structures, which corresponded in size and arrangement with the rod-shaped inclusion profiles seen in TEM sections (Fig. 1, E and F). Nile red staining and examination by light microscopy demonstrated that these inclusions were lipidic in nature (fig. S1).

Morphological similarities between the *cer5* inclusions and those found in ALD cells raised the question of whether both structures had similar composition. Because the *cer5*

inclusions could not be prepared selectively, we inferred their composition from comparisons between isolated epidermal cells with and without inclusions (3). The total fatty acid profiles of *cer5* and wild-type epidermal peels did not differ significantly. Thus, it is unlikely that the *cer5* inclusions consist of fatty acids, distinguishing them from the corresponding structures in ALD cells.

When cuticular wax components were quantified (3), wild-type plants showed a wax load of 0.24  $\mu\text{g}/\text{mm}^2$ , whereas the mutant had only 0.11  $\mu\text{g}/\text{mm}^2$  of wax (Fig. 2A). The amounts of all wax components (e.g., alkanes, ketones, and primary and secondary alcohols) on the *cer5* surface were significantly reduced (Fig. 2B). In contrast, the amounts of total epidermal wax (surface plus intracellular) extracted from isolated epidermal peels of wild type (0.31  $\mu\text{g}/\text{mm}^2$ ) and *cer5* (0.28  $\mu\text{g}/\text{mm}^2$ ), did not differ significantly. Thus, wax biosynthesis was not compromised in *cer5*, but wax components were retained within epidermal cells.

To determine the molecular basis of the *cer5* defect, we isolated the *CER5* gene by using a combination of positional cloning and insertional mutagenesis (3). Complementation of the *cer5* mutant with the wild-type *CER5* gene (At1g51500) rescued the wax-deficient phenotype (Fig. 2A). Thus, *CER5* is the At1g51500 gene encoding an ABC transporter. During cloning, we identified an additional allele of *CER5* in the Salk transfer-DNA (T-DNA) insertional mutation collection (Salk 036776) (Fig. 2A). We designated the original mutant allele *cer5-1* and the Salk 036776 allele *cer5-2*. Sequencing of the At1g51500 gene in *cer5-1* identified a point

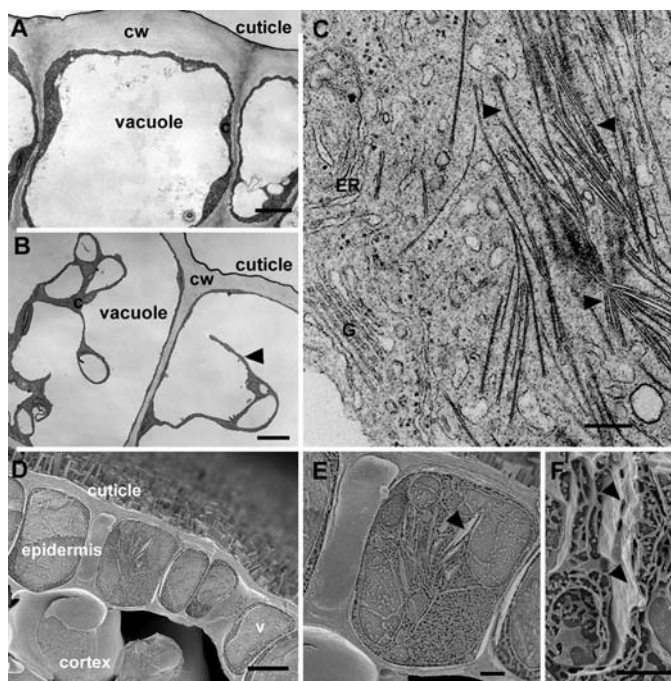


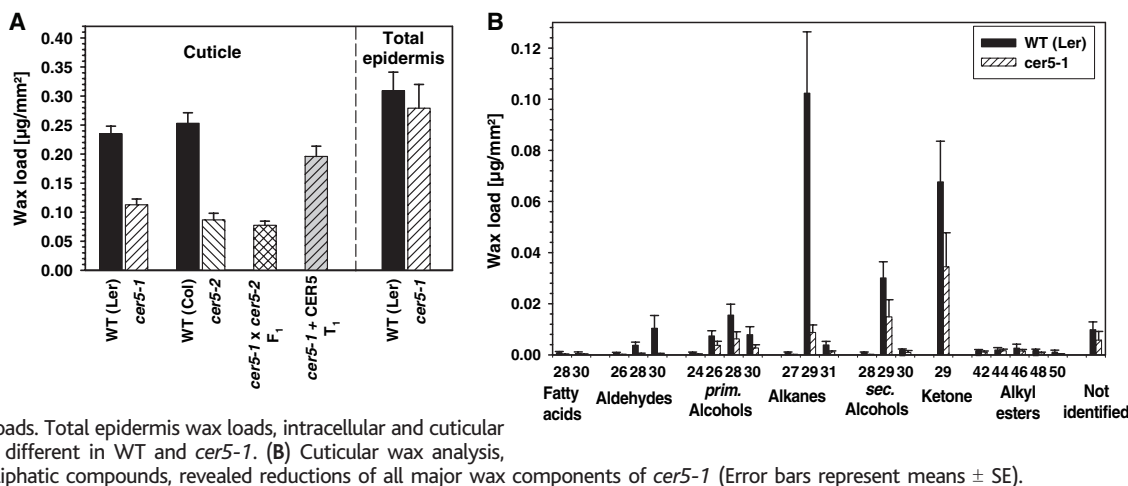
**Fig. 1.** Epidermal wax-secreting cells of *Arabidopsis* stems in transverse section. (A) Wild-type cells. c indicates cytoplasm; cw, cell wall. Scale bar, 2  $\mu\text{m}$ . (B) *cer5* cells with intrusions of cytoplasm in vacuoles (arrowhead). Scale bar, 2  $\mu\text{m}$ . (C) *cer5* cytoplasm contains unusual linear inclusions (arrowheads). ER, endoplasmic reticulum; G, Golgi. Scale bar, 200 nm. (D) Cryo-SEM of *cer5* epidermis, covered with cuticle. Scale bar, 5  $\mu\text{m}$ . (E) *cer5* epidermal cell with inclusions (arrow). Scale bar, 2  $\mu\text{m}$ . (F) High-magnification view showing sheetlike nature of inclusions. Scale bar, 2  $\mu\text{m}$ .

<sup>1</sup>Department of Botany, University of British Columbia (UBC), 6270 University Boulevard, Vancouver, BC V6T 1Z4, Canada. <sup>2</sup>Department of Chemistry, UBC, 2036 Main Mall, Vancouver, BC V6T 1Z1, Canada.

\*These authors contributed equally to this work.

†To whom correspondence should be addressed. E-mail: lsamuels@interchange.ubc.ca

**Fig. 2.** Wax analyses of *Arabidopsis* stem surface (cuticle) or epidermal peel extracts (total epidermis). (A) Cuticular wax loads of WT ecotypes are significantly different from the corresponding mutants: Landsberg *erecta* (Ler) vs. *cer5-1*; Columbia-2 (Col) vs. *cer5-2* (*t* test,  $P = 0.05$ ). F<sub>1</sub> progeny of a *cer5-1* and *cer5-2* cross had a reduced wax load similar to both parents. *Cer5-1* plants, complemented with the At1g51500 gene, showed significantly increased wax loads. Total epidermis wax loads, intracellular and cuticular (right), are not significantly different in WT and *cer5-1*. (B) Cuticular wax analysis, including chain lengths of aliphatic compounds, revealed reductions of all major wax components of *cer5-1* (Error bars represent means  $\pm$  SE).



mutation that, in the predicted CER5 protein, would cause the replacement of a glycine with an aspartate within the consensus ABC C motif (6) (fig. S2). The T-DNA insertion in the *cer5-2* allele was located in an exon encoding the region after the predicted fifth transmembrane domain of the CER5 protein. We examined *CER5* transcript levels in the *cer5* mutants to determine the extent of gene disruption in each line. Whereas the abundance of the *CER5* transcript in *cer5-1* was comparable to the wild type, no transcript could be detected in *cer5-2*, indicating that it is a transcriptional knockout (fig. S3).

Analysis of the predicted CER5 protein sequence revealed the presence of the characteristic ABC transporter domains near the N terminus, including the Walker A and B boxes and C motif for nucleotide binding and six transmembrane domains (TMD) near the C terminus (fig. S2). When compared with prototype ABC transporters, which have the TMD near the N terminus followed by the ABC domain, the ABC-TMD orientation found in CER5 would be considered a reverse arrangement. Known ABC transporters consist of two (ABC-TMD) units (7) either within one polypeptide or as two “half-transporters” making up homo- or heterodimers. *CER5* sequence predicts that it would encode a half-transporter, so presumably CER5 would require dimerization to function.

The *CER5* sequence has been designated WBC12, a member of the *white-brown complex* subfamily, in an analysis of the 129 putative ABC transporters of the *Arabidopsis* genome (8). This is the largest subfamily of ABC transporters in *Arabidopsis*, and, although some have been cloned (9), *CER5* is the only member of the subfamily that has been characterized functionally. Two other putative *Arabidopsis* ABC transporters have high similarity to *CER5*, At3g21090 (WBC 15) and At1g51460 (WBC 13) (10). Furthermore, there is similarity to two human ABC

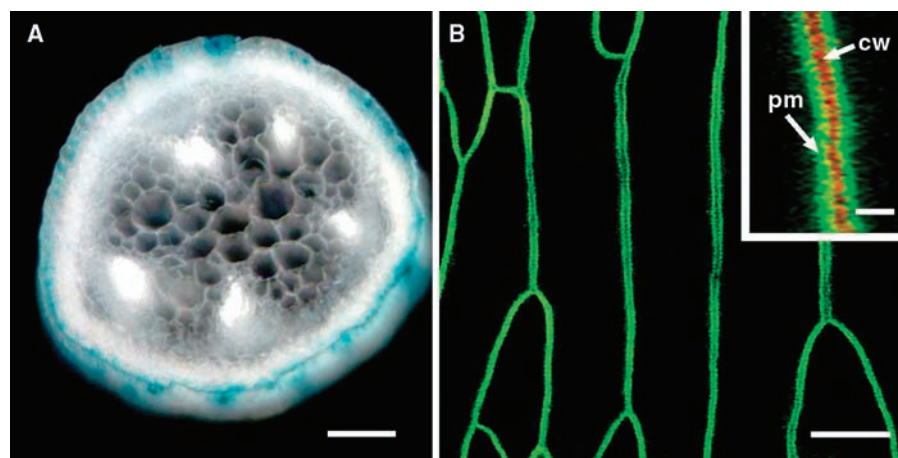


**Fig. 3.** Expression of CER5 in the plasma membrane of the stem epidermis. (A) *CER5* promoter directed epidermis-specific expression of GUS in stem. Scale bar, 100  $\mu$ m. (B) GFP-CER5 fusion protein was localized to the plasma membrane (pm) of epidermal cells. Scale bar, 10  $\mu$ m. (Inset) High magnification of GFP-CER5 expressing cells labeled with propidium iodide, which stains the cell wall red between adjacent GFP-labeled plasma membranes. Scale bar, 1  $\mu$ m.

transporters from the WBC/ABCG subfamily: breast cancer resistance protein and a placental ABCG2, which are localized to the plasma membrane (11) and believed to function in lipid and xenobiotic export (12). The simplest hypothesis is that CER5, like other WBC subfamily members, acts as a primary transporter of lipids. However, it cannot be ruled out that it acts indirectly by regulating the activities of other transporters.

*CER5* was expressed exclusively in the epidermal cells, as shown by GUS activity assays in plants transformed with the *CER5* promoter::*GUS* construct (Fig. 3A) (3). *CER5* transcript was found in all examined plant organs, including stems, leaves, siliques, flowers, and roots (fig. S4). This was unexpected, because the *cer5* phenotype is only apparent in stems or detectable by gas chromatography in stems and leaves (85% of wild-type wax load) (5). It suggests that additional transporters must be involved in delivering wax components to the cuticle in other tissues.

To investigate the subcellular localization of CER5 in *Arabidopsis*, we introduced a *GFP-CER5* (where GFP indicates green fluorescent protein) construct driven by the native *CER5* promoter into *cer5-1* plants (3). The wild-type phenotype was restored in 42 of 43 transgenic plants expressing the GFP-CER5 fusion protein, indicating that the protein was fully functional. The GFP-tagged CER5 was localized in the plasma membrane of epidermal cells (Fig. 3B). When the cell wall was stained with propidium iodide, the GFP-CER5 plasma membrane fluorescence was clearly separated by the red propidium iodide signal (Fig. 3B, inset).

We identified the plasma membrane-localized ABC transporter, CER5, involved in wax export to the plant cuticle. CER5 must be an important component of the export machinery in the *Arabidopsis* stem, because disruption of this transporter results in striking accumulations of wax inside the epidermal cells. The absence of a detectable

phenotype in tissues other than the stem and leaf and accumulation of residual surface wax on the stem of *cer5-2* knockout line suggest that additional wax export mechanisms must exist in plants. Chemical analysis of the mutant wax demonstrated that CER5, like many ABC transporters, has broad substrate specificity and is capable of transporting a variety of wax substrates. We conclude that in plants, as in other eukaryotes, proteins of the WBC/ABCG subfamily are key components of lipid transport systems.

References and Notes

1. L. Kunst, A. L. Samuels, *Prog. Lipid Res.* **42**, 51 (2003).  
 2. M. Koornneef, C. J. Hanhart, F. Thiel, *J. Hered.* **80**, 118 (1989).

3. Materials and methods are presented as supporting material on *Science Online*.  
 4. H. Powell, R. Tindall, P. Schultz, *Arch. Neurol.* **32**, 250 (1975).  
 5. A. M. Rashotte, M. A. Jenks, K. A. Feldmann, *Phytochemistry* **57**, 115 (2001).  
 6. ABC transporter motifs were predicted by PROSITE as referenced in (13).  
 7. M. Jasinski, E. Ducos, E. Martinoia, M. Boutry, *Plant Physiol.* **131**, 1169 (2003).  
 8. R. Sánchez-Fernández, T. G. E. Davies, J. O. D. Coleman, P. A. Rea, *J. Biol. Chem.* **276**, 30231 (2001).  
 9. C. T. Otsu *et al.*, *J. Exp. Bot.* **55**, 1643 (2004).  
 10. The analyses of R. Sánchez-Fernández *et al.* (8) agree with these relationships; however, they erroneously duplicated WBC15/WBC22 in their 2001 work. This was corrected in (14).  
 11. G. L. Scheffer *et al.*, *Cancer Res.* **60**, 2589 (2000).  
 12. J. W. Jonker *et al.*, *Proc. Natl. Acad. Sci. U.S.A.* **99**, 15649 (2002).  
 13. L. Falquet *et al.*, *Nucleic Acids Res.* **30**, 235 (2002).  
 14. P. A. Rea *et al.*, in *ABC Transporters from Bacteria to*

*Man*, I. B. Holland, S. P. C. Cole, K. Kuchler, C. F. Higgins, Eds. (Academic Press, London, 2003), pp. 335–355.

15. Thanks to G. Haughn, M. Smith, T. Hooker, and O. Rowland for their insightful comments. The financial support of the Natural Sciences and Engineering Research Council of Canada, Canadian Foundation for Innovation, BC Knowledge Development Foundation, and the UBC Blusson fund are gratefully acknowledged. We thank the Salk Institute for Genomic Analysis Laboratory for providing sequence-indexed *Arabidopsis* T-DNA insertion mutants (project funded by NSF). The *CER5* gene has been submitted to Genbank, and the accession no. is AY734542.

Supporting Online Material

www.sciencemag.org/cgi/content/full/306/5696/702/DC1

Materials and Methods

Figs. S1 to S4

5 July 2004; accepted 3 September 2004

# Oscillations in NF-κB Signaling Control the Dynamics of Gene Expression

D. E. Nelson,<sup>1</sup> A. E. C. Ihekweba,<sup>2</sup> M. Elliott,<sup>1</sup> J. R. Johnson,<sup>1</sup> C. A. Gibney,<sup>1</sup> B. E. Foreman,<sup>1</sup> G. Nelson,<sup>1</sup> V. See,<sup>1</sup> C. A. Horton,<sup>1</sup> D. G. Spiller,<sup>1</sup> S. W. Edwards,<sup>1</sup> H. P. McDowell,<sup>4</sup> J. F. Unitt,<sup>5</sup> E. Sullivan,<sup>6</sup> R. Grimley,<sup>7</sup> N. Benson,<sup>7</sup> D. Broomhead,<sup>3</sup> D. B. Kell,<sup>2</sup> M. R. H. White<sup>1\*</sup>

Signaling by the transcription factor nuclear factor kappa B (NF-κB) involves its release from inhibitor kappa B (IκB) in the cytosol, followed by translocation into the nucleus. NF-κB regulation of IκBα transcription represents a delayed negative feedback loop that drives oscillations in NF-κB translocation. Single-cell time-lapse imaging and computational modeling of NF-κB (RelA) localization showed asynchronous oscillations following cell stimulation that decreased in frequency with increased IκBα transcription. Transcription of target genes depended on oscillation persistence, involving cycles of RelA phosphorylation and dephosphorylation. The functional consequences of NF-κB signaling may thus depend on number, period, and amplitude of oscillations.

sized free IκBα binds to nuclear NF-κB, leading to export of the complex to the cytoplasm (10). This complex, but not free IκBα, is the target for IκBα phosphorylation by IKK (11, 12).

Oscillations in the temporal response of NF-κB activity have been observed by electromobility shift assay (EMSA) only in studies of IκBβ and ε knockout mouse embryonic fibroblast cell populations and have been simulated in a computational model (13). In the absence of time-lapse single-cell analysis, it has remained unclear whether asynchronous single-cell oscillations occur in single cells following NF-κB stimulation (8, 14). Like calcium signaling (15), NF-κB could be a complex dynamic oscillator using period and/or amplitude to regulate transcription of target genes.

We have used fluorescence imaging of NF-κB (RelA) and IκBα fluorescent fusion proteins (11, 16) to study oscillations in RelA N-C localization (N-C oscillations) in HeLa (human cervical carcinoma) cells and SK-N-AS cells [human S-type neuroblastoma cells that have been associated with deregulated NF-κB signaling (17)]. In SK-N-AS cells expressing RelA fused at the C terminus to the red fluorescent protein DsRed (RelA-DsRed) and IκBα fused at the C terminus to the enhanced green fluorescent protein EGFP (IκBα-EGFP) (Fig. 1B and Fig. 2A), 96% showed an NF-κB nuclear translocation response to tumor necrosis factor alpha (TNFα) stimulation and 72% showed long-term N-C oscillations in RelA-DsRed localization. Oscillations with a typical period of ~100 min continued for >20 hours after continuous TNFα stimulation, damping slowly. In transfected cells expressing RelA-DsRed and control EGFP (Fig. 2C), 97% responded and 91% of cells showed N-C oscillations. These oscillations appeared more synchronous between cells in the first three cycles

NF-κB is a family of dimeric transcription factors (usually RelA/p65:p50) that regulates cell division, apoptosis, and inflammation (1). NF-κB dimers are sequestered in the

cytoplasm of unstimulated cells by binding to IκB proteins. NF-κB-activating stimuli activate the inhibitor kappa B kinase (IKK) signalosome that phosphorylates IκB [at Ser32 and Ser36 on IκBα (2)] and NF-κB [at Ser536 in RelA (3, 4)]. Phosphorylated IκB proteins are then ubiquitinated and degraded by the proteasome, liberating NF-κB dimers to translocate to the nucleus and regulate target gene transcription.

IκBα is a transcriptional target for NF-κB (5), creating a negative feedback loop (Fig. 1A) in which its delayed expression gives the system similar characteristics to the circadian clock (6) and to ultradian oscillators such as p53 (7, 8) and the segmentation clock (8, 9). IκBα contains both nuclear localization and export sequences, enabling its nuclear-cytoplasmic (N-C) shuttling. Newly synthe-

<sup>1</sup>Centre for Cell Imaging, School of Biological Sciences, Bioscience Research Building, Crown Street, Liverpool, L69 7ZB, UK. <sup>2</sup>Department of Chemistry, <sup>3</sup>Department of Mathematics, University of Manchester Institute of Science and Technology, P.O. Box 88, Sackville Street, Manchester, M60 1QD, UK. <sup>4</sup>Royal Liverpool Children's National Health Service Trust, Alder Hey Hospital, Eaton Road, Liverpool, L12 2AP, UK. <sup>5</sup>Molecular Biology Department, <sup>6</sup>Advanced Science and Technology Laboratory, AstraZeneca Research and Development Charnwood, Bakewell Road, Loughborough, Leicestershire, LE11 5RH, UK. <sup>7</sup>Pfizer Central Research, Ramsgate Road, Sandwich, Kent, CT13 9NJ, UK.

\*To whom correspondence should be addressed. E-mail: mwwhite@liv.ac.uk